Journal of Molecular Spectroscopy **196,** 259–264 (1999)
Article ID jmsp.1999.7879, available online at http://www.idealibrary.com on IDEAL®

The $4^3\Pi_g$ State of Na_2: Vibrational Numbering and Hyperfine Structure

G. Lazarov,* A. M. Lyyra,*[,1] Li Li,† and J. Huennekens‡

**Department of Physics, Temple University, Philadelphia, Pennsylvania 19122; †Department of Physics and Center for Atomic and Molecular Sciences, Tsinghua University, Beijing, 100084 China; and ‡Department of Physics, Lehigh University, 16 Memorial Drive, East, Bethlehem, Pennsylvania 18015*

E-mail: Lyyra@astro.ocis.temple.edu

Received October 14, 1998; in revised form April 19, 1999

The Na_2 $4^3\Pi_g$ state has been studied by continuous-wave (cw) perturbation-facilitated optical–optical double resonance (PFOODR) fluorescence excitation and resolved fluorescence spectroscopy. The absolute vibrational numbering was determined by resolved fluorescence to the $a^3\Sigma_u^+$ state. The OODR excitation lines of the $4^3\Pi_g$ $(v, N) \leftarrow b^3\Pi_u$ $(v'_b, J') \sim A^1\Sigma_u^+$ $(v'_A, J') \leftarrow X^1\Sigma_g^+$ (v'', J'') transitions show hyperfine splittings, and the hyperfine coupling scheme of the upper $4^3\Pi_g$ levels is case $b_{\beta S}$. Although this $4^3\Pi_g$ state dissociates to the $3p + 3p$ atomic limit, it is a Rydberg state at a small internuclear distance, and the hyperfine splitting is caused mainly by the Fermi contact interaction of the $\sigma_g 3s$ valence electron with the nuclei. The Fermi contact constant was determined to be $b_F = 218.3 \pm 3.9$ MHz. © 1999 Academic Press

INTRODUCTION

The $4^3\Pi_g$ state of Na_2 has been observed recently by Liu *et al.* (*1*) using pulsed perturbation-facilitated optical–optical double resonance (PFOODR) spectroscopy. Since its development in 1983 (*2*), this method has proven to be a very powerful experimental tool in the spectroscopy of triplet states of alkali diatomic molecules. Most PFOODR experiments are based on two-step consecutive excitation and resolved fluorescence or stimulated emission pumping (SEP), starting from various levels of the thermally populated ground state. Since the ground state of all alkali dimers is of $^1\Sigma_g^+$ symmetry, transitions into triplet states are generally forbidden by the spin selection rule. The PFOODR method is based on the existence of mutually perturbed levels of the $A^1\Sigma_u^+$ and $b^3\Pi_u$ states. Because of the spin–orbit interaction, each of the two partners acquires both singlet and triplet character and thus can serve as a "gateway" (*3, 4*) or "window" (*5–8*) level through which higher excited triplet states can be reached. The $A^1\Sigma_u^+ \sim b^3\Pi_u$ perturbation has been studied experimentally and theoretically, and many mixed levels of Na_2 have been identified (*9*). We used the $A^1\Sigma_u^+$ $(v = 26) \sim b^3\Pi_u$ $(v = 28)$ window levels to study the $4^3\Pi_g$ state.

Observation of the hyperfine structure of the triplet states can provide information about the electronic structure, which in turn can be used for configuration assignment. Although the dissociation behavior can be obtained from *ab initio* calculations (*10, 11*), the configurational character might change with internuclear distance. This complicated evolution can be followed by studying the hyperfine structure of electronic states at intermediate internuclear distances. With the development of narrowband lasers, it has become possible to observe the hyperfine splitting in the excited states of various alkali diatomic molecules with great accuracy. The hyperfine structure of the $2^3\Pi_g$, $3^3\Pi_g$ (*12, 13*), $1^3\Delta_g$ (*14*), $4^3\Sigma_g^+$ (*15*), $2^3\Delta_g$ (*16*), and $b^3\Pi_u$ (*17, 18*) states of Na_2, and the $2^3\Sigma_g^+$, $3^3\Sigma_g^+$, $4^3\Sigma_g^+$ (*19, 20*), $b^3\Pi_u$, $2^3\Pi_g$, $3^3\Pi_g$ (*21*), and $1^3\Delta_g$ (*8, 20*) states of $^7Li_2$ has been resolved by cw PFOODR spectroscopy.

In this paper we report on our new experimental data which allow us to determine the absolute vibrational numbering and hyperfine structure of the $4^3\Pi_g$ state of Na_2.

EXPERIMENTAL

The experimental setup has been reported previously (*4, 9*). Sodium vapor was generated in a heat-pipe oven. Argon buffer gas was used at 1-2 Torr pressure, causing the heat pipe to operate at a temperature of about 500°C. Two single-mode, frequency-stabilized cw dye lasers were used to provide counterpropagating PUMP and PROBE beams, overlapped at the center of the heat pipe. Laser-induced fluorescence (LIF) of I_2 was used to calibrate the PUMP and PROBE laser frequencies (*22*). The PUMP laser was operated with R6G dye and its frequency was fixed on a particular $b^3\Pi_u$ $(v'_b, \Omega', J') \sim A^1\Sigma_u^+$ $(v'_A, J') \leftarrow X^1\Sigma_g^+$ (v'', J'') transition. The PROBE laser was scanned in the 18 300–18 800 cm^{-1} frequency range (Pyromethene 556 dye) to provide a second excitation step from the intermediate levels to the $4^3\Pi_g$ (v, N) levels. The OODR transitions were detected by monitoring the strong collision-induced violet $2^3\Pi_g \rightarrow a^3\Sigma_u^+$ fluorescence in the side direction (*23*) using a filtered PMT/lock-in system. A combination of

---

[1] To whom all correspondence should be addressed.

0022-2852/99 $30.00

three filters was used, and the maximum transmission was 65% at 420 nm, falling to ~1% at $\lambda > 470$ nm and $\lambda < 360$ nm. With the PUMP and PROBE laser frequencies held fixed on a particular $4^3\Pi_g$ (v, N) $\leftarrow b^3\Pi_u$ (v'_b, J') $\sim A^1\Sigma_u^+$ (v'_A, J') $\leftarrow X^1\Sigma_g^+$ (v'', J'') OODR transition, the total $4^3\Pi_g$ (v, N) $\rightarrow a^3\Sigma_u^+$ fluorescence emerging from the opposite side window of the heat-pipe oven was dispersed with a double grating monochromator (SPEX 1404) and detected with another PMT operating in the photon-counting mode.

RESULTS AND DISCUSSION

From the mixed intermediate level $b^3\Pi_u$ (v'_b, J') $\sim A^1\Sigma_u^+$ (v'_A, J'), both singlet and triplet *gerade* states can be excited. We observed the $4^3\Pi_g$, $4^3\Sigma_g^+$, $2^3\Delta_g$, and $6^1\Sigma_g^+$ states in the 35 800–36 400 cm^{-1} energy region above the potential minimum of the ground state. All these states have been previously observed (*1, 15, 16, 24*).

$4^3\Pi_g \rightarrow a^3\Sigma_u^+$ Resolved Fluorescence: Absolute Vibrational Numbering of the $4^3\Pi_g$ State

The OODR signals we report in this work were observed by monitoring the violet fluorescence while scanning the PROBE laser frequency. To distinguish transitions into triplet states from those into singlet states, we recorded OODR excitation spectra via both mutually perturbed mixed intermediate levels. The OODR signals into triplet states are stronger through the intermediate level with predominantly triplet character than through the other member of the mutually perturbing intermediate level pair with predominantly singlet character, and vice versa. This technique of triplet vs. singlet assignment is illustrated in Fig. 1. Spectrum (b) was recorded with the PUMP laser frequency held fixed to the $b^3\Pi_{1u}$ ($v' = 28$, $J' = 22$) $\leftarrow X^1\Sigma_g^+$ ($v'' = 2$, $J'' = 21$) transition. Spectrum (a) was recorded with the PUMP laser exciting the $A^1\Sigma_u^+$ ($v' = 26$, $J' = 22$) level which is the predominantly singlet member of the same mixed singlet–triplet intermediate pair. Scan (c) is identical to (b) except that it was recorded at 0.95 Torr, demonstrating the improved signal-to-noise ratio at lower pressures. Clearly, the signal at 36 240.527 cm^{-1} is due to a transition into a triplet state [assigned as $4^3\Pi_g$ ($v = 12$, $N = 21$)], while the line at 36 240.613 cm^{-1} represents a transition into a singlet state [assigned as $3^1\Pi_g$ ($v = 25$, $J = 22$); see also Ref. (*24*)].

The OODR data for the $4^3\Pi_g$ state is summarized in Table 1. Figure 2 shows the bound-free portion of the resolved fluorescence from the $4^3\Pi_g$ ($v = 12$, $N = 23$) level, with term value $T(v, N) = 36\,249.760$ cm^{-1}, to the $a^3\Sigma_u^+$ state. The fluorescence below $\lambda = 3308$ Å corresponds to transitions into the bound levels of the $a^3\Sigma_u^+$ state (not resolved in our spectrum). The PUMP and PROBE laser frequencies were held fixed on the $4^3\Pi_g$ ($v = 12$, $N = 23$) $\leftarrow b^3\Pi_u$ ($v' = 28$, $J' = 22$) $\leftarrow X^1\Sigma_g^+$ ($v'' = 2$, $J'' = 21$) transitions ($\nu_{\text{PUMP}} =$

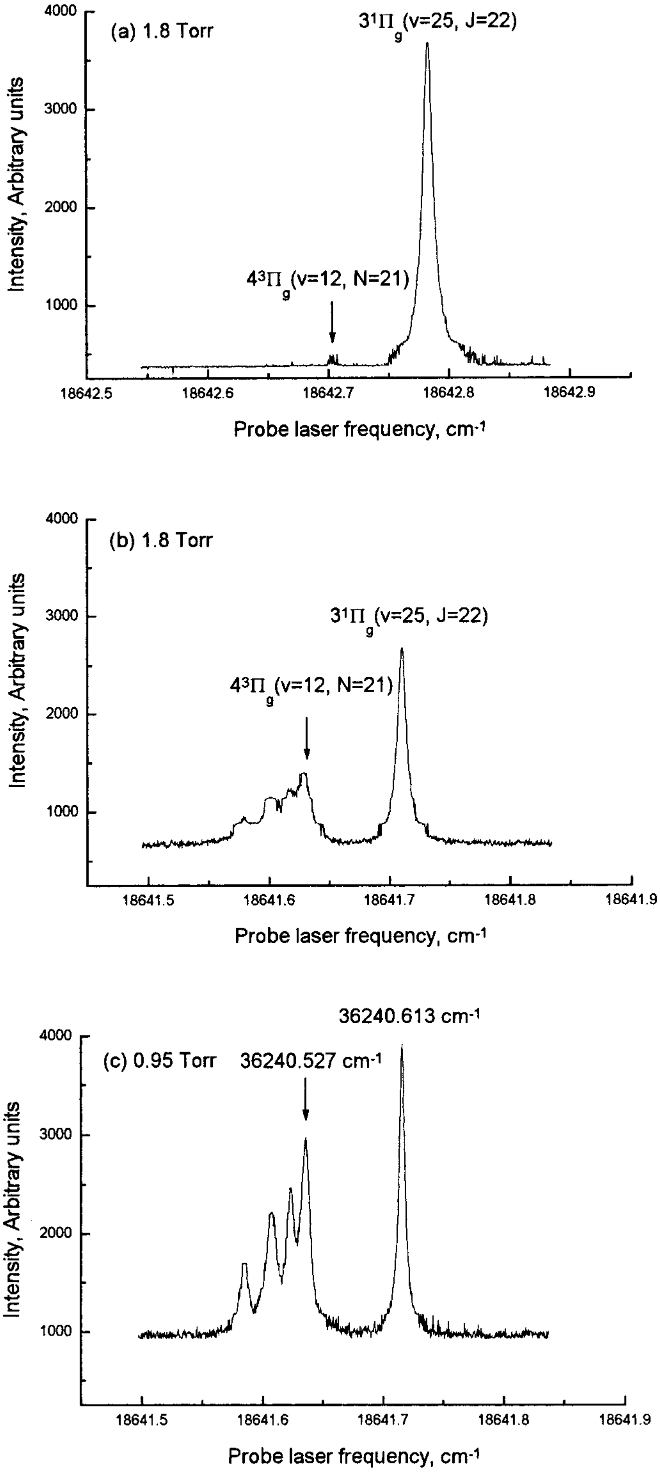

FIG. 1. Singlet vs. triplet assignment: the energy region near 36 240.6 cm^{-1} was probed via (a) the predominantly singlet $A^1\Sigma_u^+$ ($v' = 26$, $J' = 22$) level, and (b) the predominantly triplet $b^3\Pi_u$ ($v' = 28$, $J' = 22$) level. Both scans (a) and (b) were recorded with an argon buffer gas pressure of 1.8 Torr. Scan (c) is identical to (b) except that it was recorded at 0.95 Torr, demonstrating the improved signal-to-noise ratio at lower pressures.

TABLE 1
PFOODR Excitation Data for the Na_2 $4^3\Pi_g$ State

Intermediate levels				Probe laser frequency (cm^{-1})	$4^3\Pi_g$ levels		Term values (cm^{-1})	
A/b	v′	J′	Ω′		v	N	This Work	Calculated from constants of [1]
b	28	16	2	18647.948	12	14	36215.290	36214.57
				18650.370	12	15	36217.712	36217.66
				18654.073	12	16	36221.415	36220.96
				18657.218	12	17	36224.560	36224.46
				18661.406	12	18	36228.748	36228.17
A	26	22		18650.749	12	21	36240.524	36240.53
b	28	22	1	18649.670	12	21	36240.527	36240.53
				18654.901	12	22	36245.758	36245.05
				18658.903	12	23	36249.760	36249.78
				18664.726	12	24	36255.583	36254.72
b	28	28	0	18644.851	12	26	36266.207	36265.20
				18656.286	12	28	36277.642	36276.50
b	28	22	1	18750.670	13	20	36341.527	36342.93
				18756.229	13	21	36347.086	36347.22
				18761.509	13	22	36352.366	36351.72
				18765.382	13	23	36356.238	36356.43
				18771.234	13	24	36362.090	36361.33

17 127.297 cm^{-1}, $\nu_{PROBE} = 18\,658.903\ cm^{-1}$). The presence of 13 peaks (12 nodes) indicates that the correct vibrational quantum number of this upper $4^3\Pi_g$ level is $v = 12$.

Hyperfine Structure of the $4^3\Pi_g$ State

Each ^{23}Na nucleus has a nuclear spin quantum number of 3/2 (Fermi statistics). Therefore the nuclear spin quantum number of the Na_2 molecule can take values $I = 3, 2, 1$, and 0. Since the total wavefunction (including nuclear spin) has to be antisymmetric for nuclei of half-integer spin (*25*), a symmetric rotational level (the even-numbered rotational levels of the $X^1\Sigma_g^+$ state and the odd-numbered rotational levels of the $A^1\Sigma_u^+$ state) can only have antisymmetric nuclear spin wavefunctions (namely $I = 2, 0$), and an antisymmetric rotational level (the odd-numbered rotational levels of the $X^1\Sigma_g^+$ state and the even-numbered rotational levels of the $A^1\Sigma_u^+$ state) can only have symmetric nuclear spin wavefunctions (namely $I = 3, 1$). Since the rotational wavefunction symmetric ↔ symmetric, antisymmetric ↔ antisymmetric, and antisymmetric ←/→ symmetric selection rules hold rigorously for both perturbations and dipole-allowed transitions, the even- (odd) numbered rotational levels of the $b^3\Pi_u$ state perturbed by the $A^1\Sigma_u^+$ state are antisymmetric (symmetric) and the $4^3\Pi_g$ rotational levels observed via even- (odd) numbered intermediate rotational levels are also antisymmetric (symmetric). All the $4^3\Pi_g$ levels

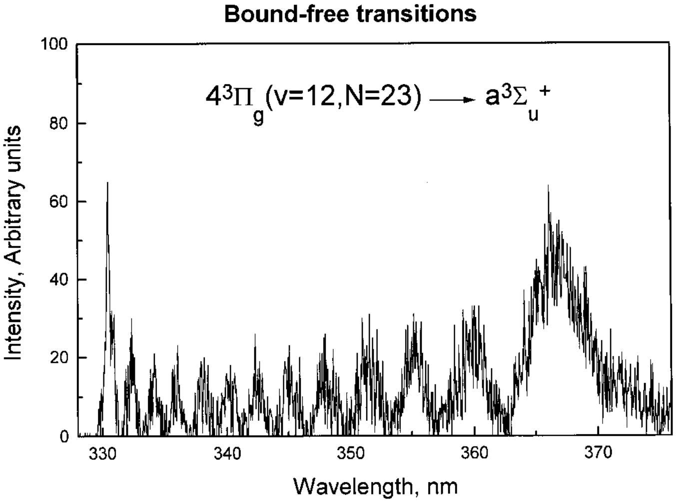

FIG. 2. $4^3\Pi_g$ ($v = 12$, $N = 23$) $\rightarrow a^3\Sigma_u^+$ resolved fluorescence. The presence of 13 peaks (12 nodes) in the bound-free fluorescence spectrum indicates that the vibrational quantum number of the upper $4^3\Pi_g$ level is $v = 12$.

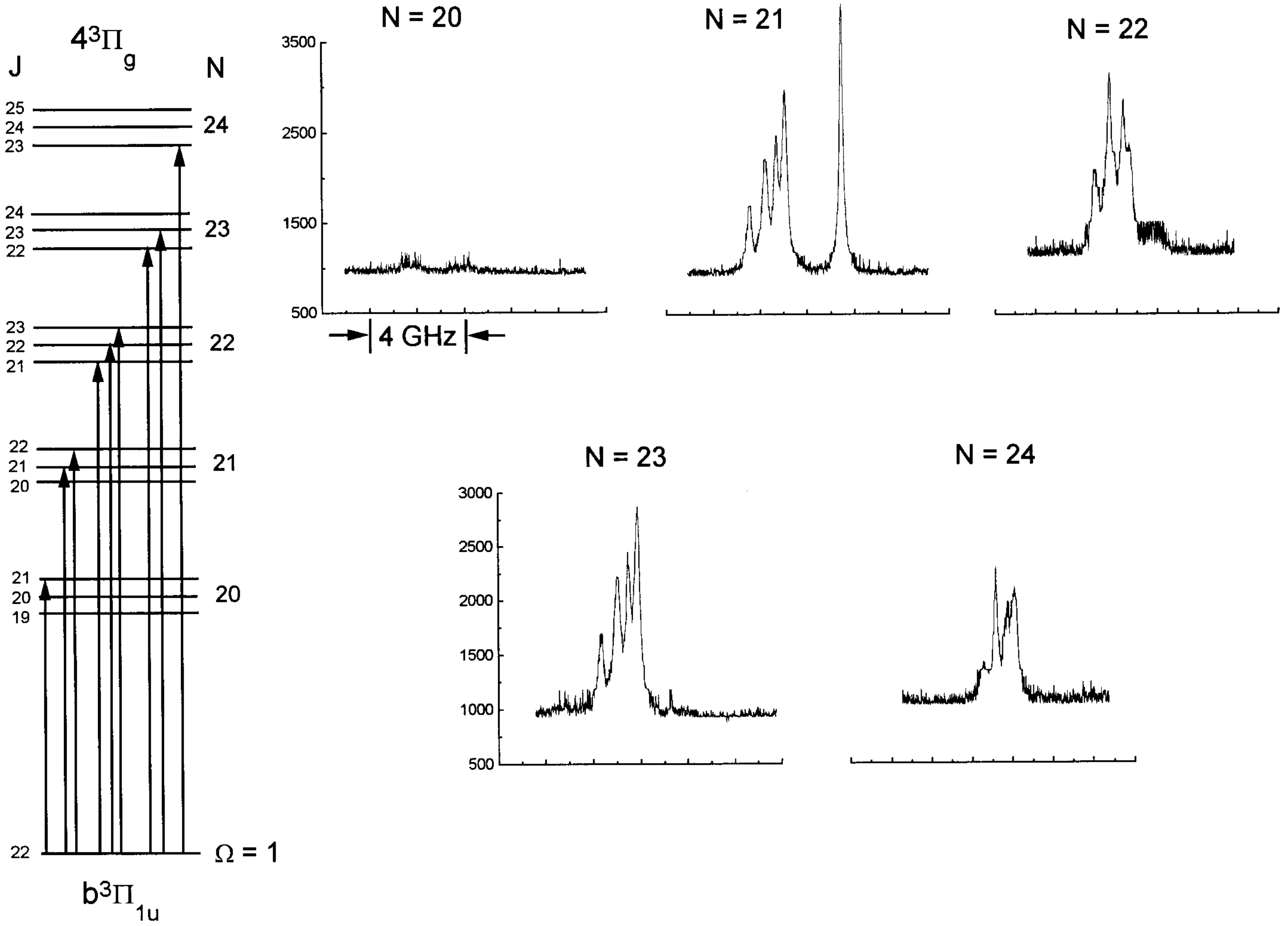

FIG. 3. OODR excitation lines of the $4^3\Pi_g$ ($v = 12$) ← $b^3\Pi_{1u}$ ($v' = 28$, $J' = 22$) transition. The sharp line on the right-hand side of the $N = 21$ panel is a transition into a singlet level, assigned as $3^1\Pi_g$ ($v = 25$, $J = 22$) (compare to Fig. 1c). The schematic energy level diagram gives a simplified picture of the transitions involved. Note, however, that J is not a good quantum number for the $4^3\Pi_g$ state. The J values in the figure are based on neglect of hyperfine structure (i.e., $J = N + S$).

studied in the present work were observed via even-J' ($J' = 16$, 22, 28), *e*-parity, *a*-symmetry intermediate levels.

For Rydberg triplet states of Na_2, the most significant term in the hyperfine Hamiltonian is the Fermi contact interaction between the nuclei and the $\sigma_g 3s$ electron (*26*), $b_F \boldsymbol{I} \cdot \boldsymbol{S}$, where b_F is the Fermi contact parameter (constant). All triplet Rydberg states of the Na_2 molecule that have been observed, except the $2^3\Pi_g$ and $3^3\Pi_g$ states, follow the case $b_{\beta S}$ hyperfine coupling scheme, in which the electronic spin $\boldsymbol{S}$ couples to the nuclear spin $\boldsymbol{I}$ to yield $\boldsymbol{G}$ ($\boldsymbol{G} = \boldsymbol{S} + \boldsymbol{I}$), and G is a good quantum number. (Note that $\boldsymbol{G}$, in turn, couples to $\boldsymbol{N}$ to form the total angular momentum $\boldsymbol{F}$; $\boldsymbol{F} = \boldsymbol{G} + \boldsymbol{N}$.) The eigenenergies in the case $b_{\beta S}$ coupling scheme are given by

$$E_{G,I,S} = (b_F/2)\,[G(G+1) - I(I+1) - S(S+1)]. \quad [1]$$

The $4^3\Pi_g$ state follows Hund's case b coupling and the intermediate $b^3\Pi_u$ state is between case a and case b. Thus five rotational lines, $N = J' - 2$, $J' - 1$, J', $J' + 1$, $J' + 2 \leftarrow J'$ (*O*, *P*, *Q*, *R*, and *S* lines), are expected. Figure 3 shows the five lines of the $4^3\Pi_g$ ($v = 12$) ← $b^3\Pi_{1u}$ ($v' = 28$, $J' = 22$) transition. If the $4^3\Pi_g$ state follows the case $b_{\beta S}$ hyperfine coupling scheme, there will be six $G(= I + S, I + S - 1, \ldots, I - S)$ components within every N level: $G = 4, 3, 2$ for $I = 3$, and $G = 2, 1, 0$ for $I = 1$ (in Ref. (*12*) it is shown that the $G = 3$, $I = 3$ component overlaps in energy with the $G = 1$, $I = 1$ component, and therefore only five distinct hyperfine components should be observable in each rotational line). The OODR excitation lineshapes for transitions into the $4^3\Pi_g$ state are very similar to those previously observed for transitions into the $1^3\Delta_g$, $2^3\Delta_g$, and $4^3\Sigma_g^+$ Rydberg states of Na_2 (*14–16*). In Fig. 4 we compare signals for the $4^3\Pi_g$ ($v = 12$, $N = 26$) and $2^3\Delta_g$ ($v = 25$, $N = 22$) levels, excited via $b^3\Pi_{0u}$ ($v' = 28$, $J' = 28$) and $b^3\Pi_{1u}$ (v'

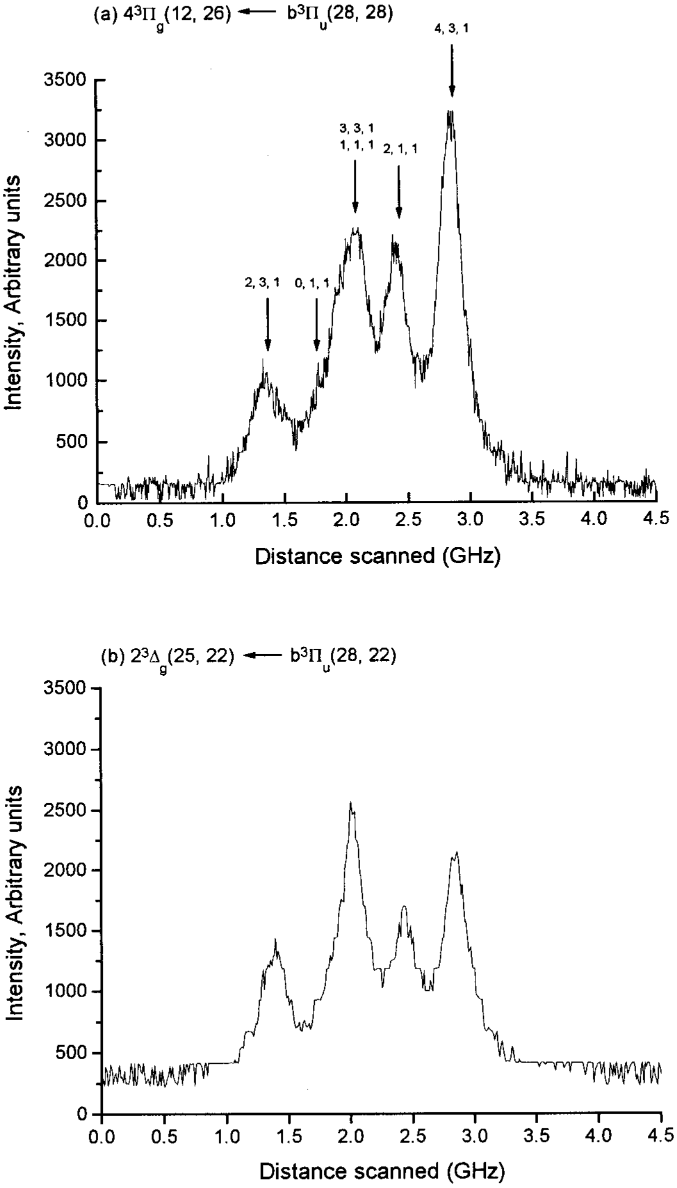

FIG. 4. PFOODR excitation spectra of (a) the $4^3\Pi_g$ ($v = 12$, $N = 26$) $\leftarrow$ $b^3\Pi_{0u}$ ($v' = 28$, $J' = 28$) and (b) the $2^3\Delta_g$ ($v = 25$, $N = 22$) $\leftarrow b^3\Pi_{1u}$ ($v' = 28$, $J' = 22$) transitions. In (a) the hyperfine components are labeled by the *G, I, S* quantum numbers.

$= 28$, $J' = 22$) intermediate levels, respectively. Clearly, the two spectra show the same pattern, suggesting that the two upper states have the same coupling scheme. The $2^3\Delta_g$ state follows the case $b_{\beta S}$ hyperfine coupling scheme (*16*). Therefore, it is reasonable to characterize the $4^3\Pi_g$ state with the same $b_{\beta S}$ coupling case.

The energies of the $4^3\Pi_g$ level hyperfine components, $E_{G,I,S}$, can be calculated from Eq. [1] and are $E_{4,3,1} = 3b_F$, $E_{3,3,1} = E_{1,1,1} = -b_F$, $E_{2,3,1} = -4b_F$, $E_{2,1,1} = b_F$, $E_{0,1,1} = -2b_F$. Thus the energy differences between the hyperfine components are (from lower to higher energy) $2b_F$, b_F, $2b_F$, $2b_F$; the second peak being very weak. The hyperfine splitting of the $b^3\Pi_{1u}$ state is unresolvable at a resolution of 15 MHz (*17*). The $b^3\Pi_{0u}$ and $b^3\Pi_{2u}$ states have larger magnetic hyperfine splittings. However, in the counterpropagating PUMP and PROBE laser geometry used in this work, the Doppler shift of the different hyperfine structure components of the intermediate state is, for the most part, canceled (*12, 27*), and the hyperfine structure of the OODR signals in Figs. 3 and 4 is mainly due to the upper level splitting. The value of the Fermi contact parameter, as measured from 10 experimental OODR spectra with well-resolved hyperfine structure (based on the $2b_F$, b_F, $2b_F$, $2b_F$ pattern described above) is $b_F = 218.3 \pm 3.9$ MHz. This value is in excellent agreement with the one predicted by Li Li *et al.* (*14*):

$$b_F(4\,^3\Pi_g, \mathrm{Na_2}) = (1/4)b_F(3\,^2\mathrm{S}, \mathrm{Na}) = 221.5 \text{ MHz},$$

where $b_F(3^2\mathrm{S}, \mathrm{Na}) = 886$ MHz for the free atom ^{2}S ground state (*28*).

Although *ab initio* calculation predicts that the $4^3\Pi_g$ state dissociates adiabatically to the $3p + 3p$ atomic limit, it has a Rydberg character at a smaller internuclear distance (*1, 11*). The fact that the $4^3\Pi_g$ state follows case $b_{\beta S}$ hyperfine coupling and its hyperfine constant is similar to other Na_2 Rydberg triplet states indicates that this state has a $\sigma_g 3s$ valence orbital character and therefore can be classified as a Rydberg state in the range of internuclear separations probed by this experiment.

SUMMARY

The $4^3\Pi_g$ state of Na_2 has been studied by cw PFOODR spectroscopy. The absolute vibrational numbering has been determined. The hyperfine structure of the $4^3\Pi_g$ state has also been measured, and the Fermi contact parameter has been reported. The case $b_{\beta S}$ hyperfine coupling scheme and 218 MHz Fermi contact constant indicate that the $4^3\Pi_g$ state can be classified as a Rydberg state in our observation region, although it adiabatically dissociates to the $3p + 3p$ atomic limit.

ACKNOWLEDGMENTS

We thank X. Wang, J. Yang, and J. Qi for experimental assistance. This research was supported by a grant from the National Science Foundation.

REFERENCES

1. Y. Liu, H. Chen, J. Li, D. Chen, L. Li, and R. W. Field, *J. Mol. Spectrosc.* **192,** 32–40 (1998) [and references therein].
2. L. Li and R. W. Field, *J. Phys. Chem.* **87,** 3020–3022 (1983).
3. W. M. Gelbart and K. F. Freed, *Chem. Phys. Letts.* **18,** 470–475 (1973).
4. Li Li, Q. Zhu, A. M. Lyyra, T.-J. Whang, W. C. Stwalley, R. W. Field, and M. H. Alexander, *J. Chem. Phys.* **97,** 8835–8841 (1992).
5. A. Yiannopoulou, K. Urbanski, A. M. Lyyra, Li Li, B. Ji, J. T. Bahns, and W. C. Stwalley, *J. Chem. Phys.* **102,** 3024–3031 (1995).
6. X. Xie and R. W. Field, *J. Mol. Spectrosc.* **117,** 228–244 (1986).
7. X. Xie and R. W. Field, *Chem. Phys.* **99,** 337–345 (1985).

8. Li Li, T. An, T.-J. Whang, A. M. Lyyra, W. C. Stwalley, R. W. Field, and R. A. Bernheim, *J. Chem. Phys.* **96,** 3342–3343 (1992).
9. T.-J. Whang, W. C. Stwalley, L. Li, and A. M. Lyyra, *J. Chem. Phys.* **97,** 7211–7219 (1992) [and references therein].
10. G. H. Jeung, *J. Phys. B: At. Mol. Phys.* **16,** 4289–4297 (1983).
11. S. Magnier, Ph. Millié, O. Dulieu, and F. Masnou-Seeuws, *J. Chem. Phys.* **98,** 7113–7125 (1993).
12. Li Li and R. W. Field, *J. Mol. Spectrosc.* **117,** 245–282 (1986).
13. Li Li and R. W. Field, *J. Mol. Spectrosc.* **123,** 237–246 (1987).
14. Li Li, Q. Zhu, and R. W. Field, *J. Mol. Spectrosc.* **134,** 50–62 (1989).
15. Li Li, Q. Zhu, and R. W. Field, *J. Mol. Phys.* **66,** 685 (1989).
16. T.-J. Whang, A. M. Lyyra, W. C. Stwalley, and Li Li, *J. Mol. Spectrosc.* **149,** 505–511 (1991).
17. J. B. Atkinson, J. Becker, and W. Demtröder, *Chem. Phys. Letts.* **87,** 128–133 (1982).
18. H. Katô, M. Otani, and M. Baba, *J. Chem. Phys.* **89,** 653–659 (1988).
19. A. Yiannopoulou, K. Urbanski, S. Antonova, A. M. Lyyra, Li Li, T. An, B. Ji, and W. C. Stwalley, *J. Mol. Spectrosc.* **172,** 567–572 (1995).
20. A. Yiannopoulou, K. Urbanski, A. M. Lyyra, Li Li, B. Ji, J. T. Bahns, and W. C. Stwalley, *J. Chem. Phys.* **102,** 3024–3031 (1995).
21. Li Li, A. Yiannopoulou, K. Urbanski, A. M. Lyyra, B. Ji, W. C. Stwalley, and T. An, *J. Chem. Phys.* **105,** 6192–6199 (1996).
22. S. Gerstenkorn and P. Luc, "Atlas du Spectre D'Absorption de la Molecule d'Iode," Presses du CNRS, Paris, 1978.
23. [Collision-induced $2^3\Pi_g \rightarrow a^3\Sigma_u^+$ fluorescence was much stronger than the direct $4^3\Pi_g \rightarrow a^3\Sigma_u^+$ fluorescence for our experimental conditions. Collision-induced $2^3\Pi_g \rightarrow a^3\Sigma_u^+$ fluorescence was also monitored when exciting to other triplet and singlet states.]
24. C.-C. Tsai, J. T. Bahns, and W. C. Stwalley, *J. Mol. Spectrosc.* **167,** 429–436 (1994); A. J. Taylor, K. M. Jones, and A. L. Schawlow, *Opt. Commun.* **39,** 47–50 (1981).
25. G. Herzberg, "Molecular Spectra and Molecular Structure, Volume I, Spectra of Diatomic Molecules," Krieger, Malabar, FL, 1989.
26. R. A. Frosch and H. M. Foley, *Phys. Rev.* **88,** 1337–1349 (1952).
27. Li Li, Q. Zhu, A. M. Lyyra, T.-J. Whang, W. C. Stwalley, R. W. Field, and M. H. Alexander, *J. Chem. Phys.* **98,** 8413–8418 (1993).
28. P. Kusch and V. W. Hughes, *in* "Handbuch der Physik" (S. Flügge, Ed.), Vol. 37, Part I, pp. 100 and 117, Springer-Verlag, Berlin, 1959; C. K. Jen, V. A. Bowers, E. L. Cochran, and S. N. Foner, *Phys. Rev.* **126,** 1749–1757 (1962); W. Hartig and H. Walther, *Appl. Phys.* **1,** 171 (1973).